

THE PROBA SATELLITE STAR TRACKER PERFORMANCE

John Leif Jørgensen¹⁾, Troelz Denver²⁾, Maurizio Betto³⁾,
Pieter Van den Braembussche⁴⁾

¹⁾, ²⁾, ³⁾ Technical University of Denmark, Dept. of Measurement and Instrumentation,
Building 327, DK-2800 Lyngby, Denmark.

¹⁾ +45 45253448, jlj@oersted.dtu.dk

⁴⁾ VERHAERT Design & Development, Hogenakkerhoekstraat 21,
B-9150 Kruikebeke, Belgium, +32 32501909, pieter.vdb@verhaert.com

ABSTRACT

ESA's PROBA satellite features a high degree of autonomy. The science missions of PROBA call for high pointing accuracy and high agility. The Advanced Stellar Compass (ASC) provides the pointing knowledge with accuracy in the arc second range. A description of the PROBA ASC is given and various aspects of the ASC are treated: Handling of solar and lunar blinding, tolerance to dark and lit Earth horizons in the field of view and measurement accuracy. Investigation of the Inter Boresight Angle demonstrates that the spacecraft has thermal flexures, which can be modeled down to a few arc seconds. Finally timing and radiation issued for the ASC are treated.

1. INTRODUCTION

The Project for OnBoard Autonomy, PROBA, satellite, is ESA's first full scale demonstration of what can be achieved, technologically as well as scientifically, using onboard autonomy for almost any satellite function. The PROBA satellite is a true micro satellite, with a mass of 94kg and a size of only 800mm by 600mm by 600mm. The mission is build up around a powerful onboard command, data and AOCS controller unit, that handles all TM/TC functions, scheduling as well as the top level autonomous control. But it also implements other novelties such as gyro-free attitude control and a high pointing accuracy coupled with a very high agility.

One of the main scientific goals for the mission is to measure the Spectral Bidirectional Reflectance Distribution Function, BRDF, of vegetation types and landscape, the measurement of which is performed by a scanning telescope. Since the BRDF requires measurement of the same target from all viewing and illumination angles, the satellite needs to be very agile to be able to point the telescope at the target during the flyby, from it rises over the horizon till it sets behind. During such a maneuver 5 scans are performed of the target.

The main scientific goals for the mission also include acquisition of monochrome images of ground targets with an on-ground resolution of 4m. During such a maneuver, the line of sight of the camera pointing the target is fixed. These classical spy satellite maneuvers have to be performed with an accuracy of 5 arcseconds to ensure image quality and correct unfolding of the BRDF.

The attitude control system is consequently using a relatively powerful quad momentum wheel with magnetorquer dumping system, and a fully autonomous star tracker system for the inertial attitude reference. The selected star tracker system was the fully autonomous Advanced Stellar Compass, the ASC.

2. THE PROBA STAR TRACKER

Since the science goal for PROBA requires the satellite to operate at large slant angles relative to the local vertical, it is inevitable that the boresight of any single star tracker is brought to bear under the Earth horizon, this obviously will impair proper operations. It was consequently decided to use an offset configuration of the two Camera Head Units', CHU's, of 50 deg. The actual configuration of the boresights is depicted in fig. 1.

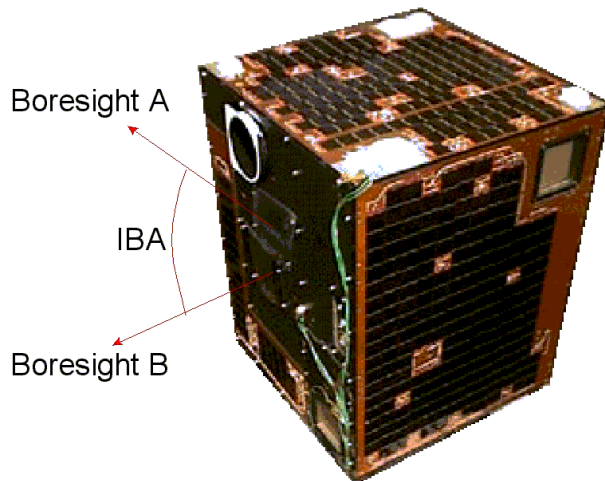


Figure 1: The PROBA Satellite. The boresights of the two CHUs are marked with arrows.

The theoretical exclusion angles are showed on fig. 2. Sunlight will start to impact proper operations at a level of about 6.3×10^{-6} .

The ASC configuration chosen for PROBA, is a fully cold redundant Data Processing Unit, DPU, attached to two CHU's via a cross strapping board. This way, either DPU may run zero, one or two CHU's. Typically only one DPU will be powered running both CHU's. Since each DPU has the capacity to generate 5.5 true solutions per second, i.e. true accurate attitude fixes per second, and since a small closed loop time is essential for support of the agility required, an update rate of 2Hz per CHU has been baselined.

The ASC itself support a wide range of integration times. Longer integration times increase the accuracy of the attitude at the cost of timeliness and vice-versa, but shorter integration times also support higher attitude change rates. Real-sky tests show that the maximum permissible rate at 2Hz is about 2.5deg/sec for >99% validity of the attitude fixes, which leaves ample margin for the PROBA mission profile.

3. HANDELING OF SUN AND MOON BLINDING

Usually the first few days of operation of a spacecraft offer plenty of opportunity to verify operations of a star tracker close to the Sun, but in the case of PROBA, the

The chosen angle between the boresights of the CHU's has another benefit: It allows for using a small straylight suppression systems, i.e. baffles, for the cameras, since the ASC recovers from direct sun blinding in a few seconds, and since simultaneous blinding is precluded by the geometry. Consequently the baffles used are extremely compact. The straylight performance of the baffles is obviously affected by the size, but as the forward/inverse Monte Carlo simulation shows, the goal of no simultaneous Sun blinding was achievable with ample margin.

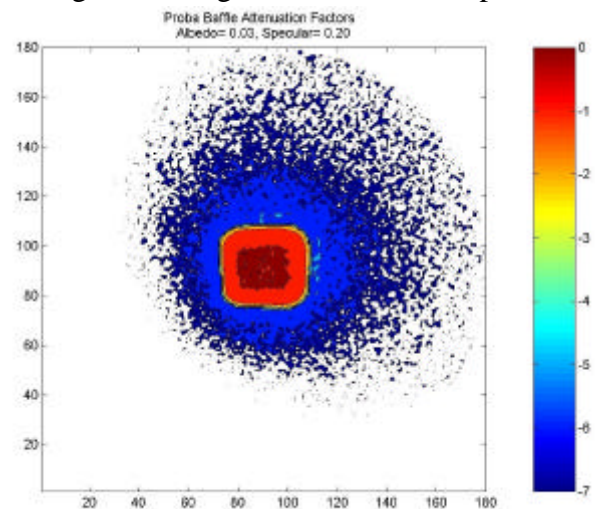


Figure 2: Monte Carlo simulation of one of the PROBA baffles. The graph shows the attenuation color-coded as function of incident angle.

autonomy has made our data from vistas of regions close to the Sun very scarce. The standard rate-damping- and safe-mode furthermore has the elegant property built, that the spacecraft always end up with the CHU's pointing more than 90 deg from the Sun. Therefore our best assessment of the Sun handling comes from scheduled maneuvers that brings one or the other boresight close to the Sun. From such orbits it is found, that the baffles are more than sufficient to handle solar blinding, and that the impact from sunlight follows the predictions from the Monte Carlo simulations closely. The basic performance is shown on fig. 3, where the Sun location, as seen from the boresight of the CHU's are plotted during a series of maneuvers.

The Moon will degrade proper operations of the ASC, when more than 75% full and fully inside the Field Of View, FOV. Since PROBA is in a fixed 10.30 polar orbit, with the cameras tilted 25E up from the orbital plane, a more than 75% Moon will pass through the field of view of either CHU every orbit, a couple of days per month. However, since the angle between the boresights precludes simultaneous lunar intrusion, operational degradations have not been noticed. ASC data from lunar passages of the FOV show the expected behavior: An attitude stream of high quality fixes, interspersed with "zero-fixes"; the signature of a slight processor overload from the processing of complex straylight influenced images.

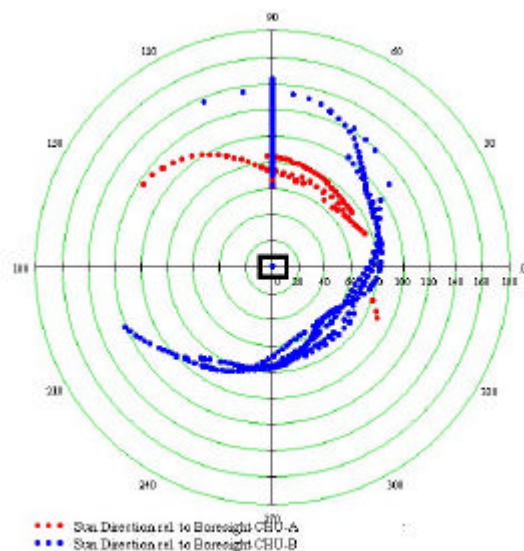


Figure 4: Polar plot of sun direction versus boresight during a couple of satellite maneuvers. The FOV is marked with a rectangle in the center of the plot.

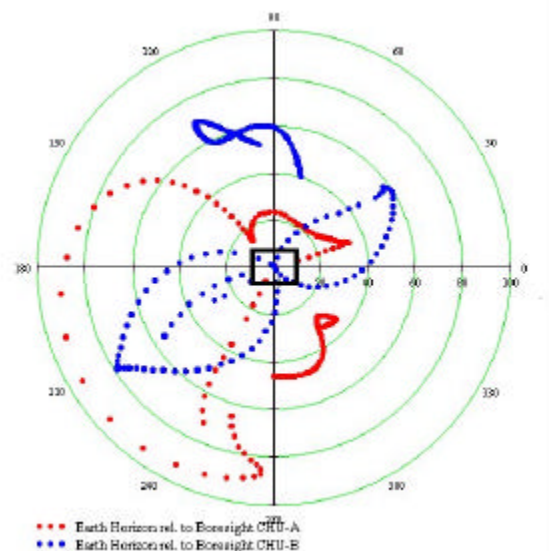


Figure 3: Polar plot of closest point on the dark Earth horizon versus boresight during a couple of satellite maneuvers. The FOV is marked with a rectangle in the center of the plot.

4. EARTH BLINDING

A far bigger concern than the Moon, is the handling of the Earth intrusion into the FOV, since the mission plan for having, routinely, the sunlit Earth inside one or the other FOV. The issue here is, that these blindings occur under circumstances where the attitude rate of change is high and where the accuracy requirements are at the highest, i.e. during science observations passing a target on the ground.

From operations of the ASC during periods with the satellite in safe mode, where the satellite is minimizing the measured dB/dt, i.e. making approximately two cartwheel rotations per orbit, it is found that the horizon of the dark Earth may come all the way to the boresight, before operations degraded, i.e. more than half the FOV is blocked by

dark Earth and the atmosphere. This is shown at fig. 4, where the closest point of dark Earth horizon relative to the FOV is plotted.

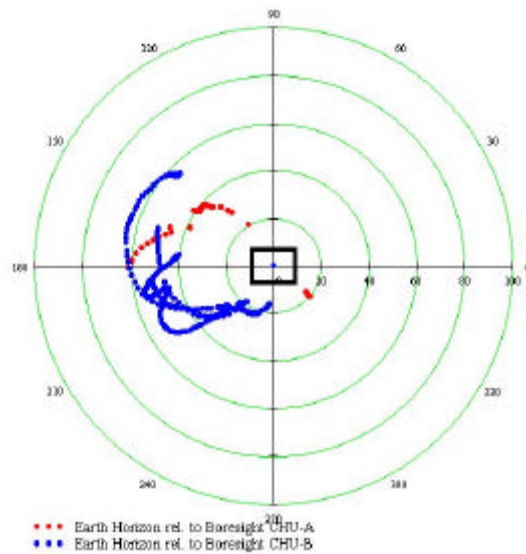


Figure 5: Polar plot of the closest point on the bright (sun-lit) Earth horizon versus boresight during a couple of satellite maneuvers. The FOV is marked with a rectangle in the center of the plot.

Similarly from safe mode, the performance with the bright Earth close to the FOV is found. Here valid updates from the CHU affected ceases, when the sunlit horizon approaches the FOV and resumes at the juxtaposed horizon leaves the other side of the FOV thus ending the blinded phase. This is showed in fig. 5, where the location of bright Earth horizon relative to the FOV, for valid updates is shown. Also shown is an outline of the location of the camera FOV.

This performance is somewhat better than what was expected from the Monte Carlo straylight analysis which showed that the bright Earth horizon will start to interfere when closer than 3-15E to the FOV, depending on which side due to the asymmetric baffle shape as shown on fig. 2.

Later, during nominal operations, it has been found that the proximity of the bright Earth indeed influences the performance, it

is just suppressed by the internal autonomy of the ASC: During nominal operations, the boresights are pointed well away from the Sun, and up from the horizon some 50E. The Earth albedo reflected light will therefore illuminate the part of the baffle protruding the farthest due to its asymmetric shape. Light from this region may statistically make it to the lens with an intensity that may interfere with proper operations. This has indeed been found to be the case, as the number of detected objects increase significantly, when the spacecraft is out of eclipse. However since the ASC is capable of handling multiple false stellar-like objects while maintaining proper operations, the only effect seen from the AOCS system is a slight increase in the processing time (processing time spent suppressing the straylight), and interspersed “zero-attitudes” (processor overload when the straylight influence increases).

5. ATTITUDE ACCURACY

Because the spacecraft attitude will change from even minute disturbance torques, and because the accuracy of the ASC is in the range of an arcsecond at 2Hz, it is virtually impossible to assess the true accuracy performance of the system using the attitude from a star camera alone. However, at missions carrying more than one CHU, the accuracy and stability may be measured simply by comparing the measurement of the individual CHU's. This is possible, since the attitude calculations are entirely independent. The only common information to the attitude from two CHU's is the clock used to time the acquisition. The clock may, however, be verified against an external reference. In the case of PROBA, where the CHU's operate on disjunct set of stars, any given set of attitudes contain all possible noise terms, and by monitoring the development in the relative attitude over time, the noise and bias terms may be characterized via direct measurement.

In the case of micro satellites, and hence PROBA, thermal distortions typically dominate, unless special focus has been put on making the mounting structure thermo-elasticly stable, i.e. an optical bench. In the case of PROBA a typical thermal swing over the orbit is about 80K externally and up to 30K internally. Since the separation structure in the bottom side precludes mounting of solar cells here, most of this temperature swing originates from a larger thermal gradient from orbital illumination differences. The honeycomb structure used consequently will react to this gradient, with a cyclic, orbital, excursion pattern around the thermal equilibrium state.

6. THE ABERRATION CORRECTION

We had the chance to analyze this pattern during the verification of the autonomous correction for the astronomical aberration effect on the attitude fixes. A simple measure of the accuracy of the ASC onboard PROBA, is the measured angle between the two boresights, the Inter-Boresight Angle, IBA. Ideally the IBA is a constant, but since the relativistic aberration is dependent of the angle between the boresight and the heliocentric velocity, since this angle is different for the two CHU's, and since this angle vary over the orbit, the IBA will also vary, if the aberration is not corrected for. Fig. 6, shows the theoretical IBA variation over the orbit for the time of test.

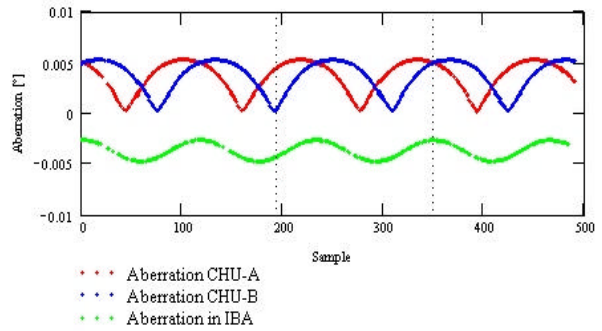


Figure 6: Theoretical aberration Correction.

The proper operation of the aberration correction was verified, simply by enabling it for a couple of orbits, then disabling it for another few orbits, and then enabling it again. By comparing the change in the IBA with the correction on and off with the theoretical results correct operations was verified, as shown on fig. 7.

The almost sinusoidal oscillations present in the measurements of fig. 7, are caused by the aforementioned orbit induced thermal gradient. Due to the fixed local time of the orbit, the thermal loading of the spacecraft has remained constant during the mission. It is nevertheless remarkable, that the orbital IBA variations have remained stable too, to an extent where it, if the model function is subtracted, is stable within a few arcseconds.

This indicates, that despite the PROBA instrument platform is not optimized for thermo-elastic stability, it may still be used for missions requiring very low platform biases. By subtracting the thermo-elastic model from the IBA data, the IBA vs. time graph shown in the bottom panel of fig. 8 is arrived at.

7. TIMING AND RADIATION

The attitude timeliness is of essence for all AOCS uses, but it must especially be kept within tight bounds for agile systems. The timestamp of the attitudes of the ASC refer to the center of integration, thus assuming no, or low, accelerating rates in the attitude.

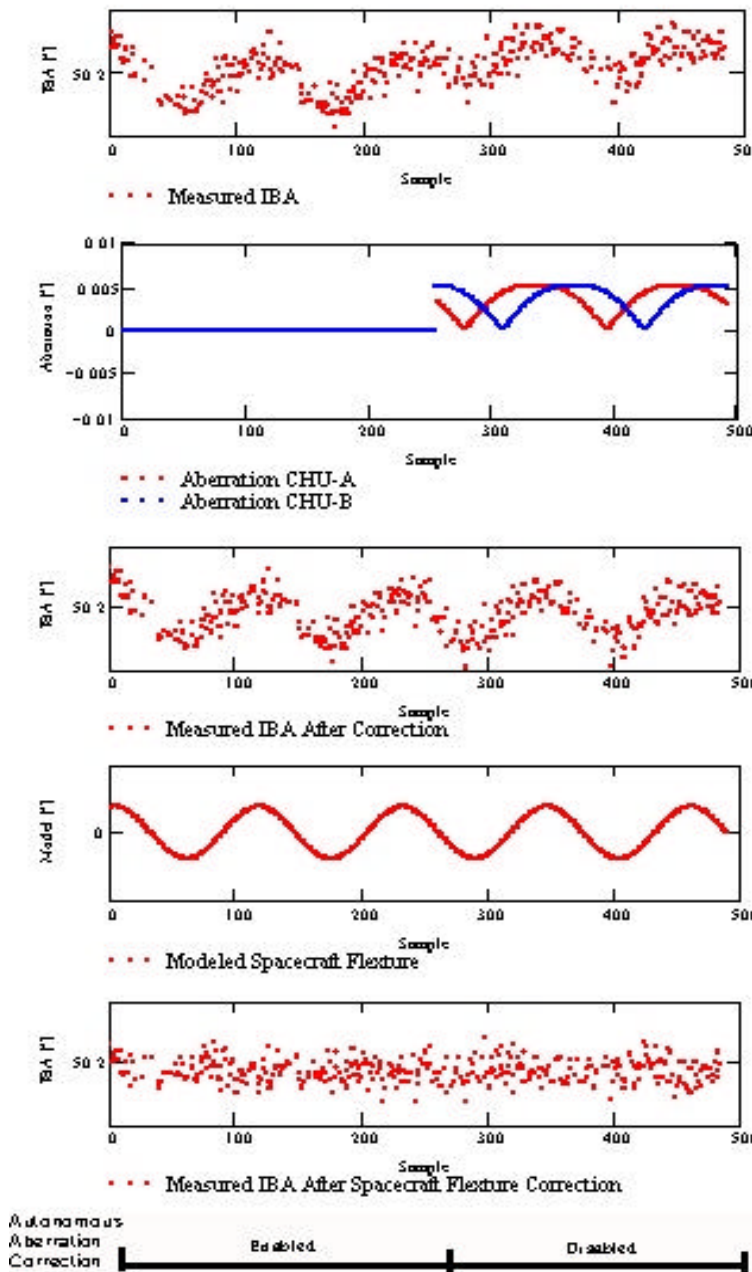


Figure 7: Plot from the aberration correction test. The autonomous on-board correction is disabled at sample 254. The second plot shows the theoretical aberration corrections for the two CHUs. The third plot shows the obtained attitude series, when on-ground aberration correction has been performed on the last half of the series. The fourth graph shows a sine model of the spacecraft flexure. The bottom graph shows the IBA after subtraction of the flexure model.

pointed further away from Earth. Since this geometry removes straylight from the outwards pointing CHU, excellent performance has been observed during observations. The attitude rate of changes incurred by the science observations, ranges between 0.3 to 0.75°/s. The ASC has proved capable of delivering high accuracy attitude at all rates and acceleration patterns tested.

After end of integration, the image is read from the CCD by the processing unit. Then the image is sifted for bright objects, larger light regions (straylight), is identified and excluded, the remaining objects are centroided. The centroid list is then matched against the star catalogue, and the least square fit, if proper, output as the attitude. This process nominally takes, from center of integration till output from the DPU, 700 ms.

PROBA has, during its mission so far, sustained several severe solar mass ejections during the past solar max. These events combined with the general radiation level from the orbit flown, has resulted in a substantial radiation dose to the electronics onboard. The impact on the operations of the ASC is mainly an increase in processing load and time, from the extra burden of filtering out the hot spots that the radiation induces in the CCD. Combined with the aforementioned straylight from bright earth, the timeliness of the attitudes has been slightly above the planned values, ranging between 800-1000. This increase originates from the PROBA/ASC configuration, treating both CHU solutions simultaneously.

Because science observations requires the satellite to track a point on Earth beneath, either one or the other boresight is pointed closer, whereas the other is